



Published in final edited form as:

*Sci Signal.* ; 9(419): ra29. doi:10.1126/scisignal.aad5578.

## Loss of Reelin protects against atherosclerosis by reducing leukocyte-endothelial adhesion and lesion macrophage accumulation

Yinyuan Ding<sup>1,2,3,\*</sup>, Linzhang Huang<sup>4,\*</sup>, Xunde Xian<sup>1,2,\*</sup>, Ivan S. Yuhanna<sup>4</sup>, Catherine R. Wasser<sup>1,2</sup>, Michael Frotscher<sup>5</sup>, Chieko Mineo<sup>4</sup>, Philip W. Shaul<sup>4,†</sup>, and Joachim Herz<sup>1,2,6,7,8,†</sup>

<sup>1</sup>Department of Molecular Genetics, UT Southwestern Medical Center, Dallas, TX 75390, USA.

<sup>2</sup>Center for Translational Neurodegeneration Research, UT Southwestern Medical Center, Dallas, TX 75390, USA.

<sup>3</sup>Key Laboratory of Medical Electrophysiology, Ministry of Education of China, and the Institute of Cardiovascular Research, Sichuan Medical University, Luzhou 646000, China.

<sup>4</sup>Center for Pulmonary and Vascular Biology, Department of Pediatrics, University of Texas Southwestern Medical Center, Dallas, TX 75390, USA.

<sup>5</sup>Zentrum für Molekulare Neurobiologie, Falkenried 94, 20251 Hamburg, Germany, Germany.

<sup>6</sup>Department of Neuroscience, UT Southwestern Medical Center, Dallas, TX 75390, USA.

<sup>7</sup>Department of Neurology and Neurotherapeutics, UT Southwestern Medical Center, Dallas, TX 75390, USA.

<sup>8</sup>Center for Neuroscience, Department of Neuroanatomy, Albert-Ludwigs-University, Freiburg 79085, Germany.

†Corresponding authors: Philip.Shaul@UTSouthwestern.edu (P.W.S.); Joachim.Herz@UTSouthwestern.edu (J.H.).

\*These authors contributed equally to this work.

### Supplementary Materials

**Fig. S1.** Induction of systemic Reelin deficiency in mice by tamoxifen injection and analysis of plasma lipids.

**Fig. S2.** Generation of mice with Reelin deficiency in the circulation using adenoviral delivery of Cre recombinase.

**Fig. S3.** Plasma Reelin abundance in chow-fed or high cholesterol diet-fed mice.

**Fig. S4.** Effect of plasma Reelin absence on macrophage accumulation in atherosclerotic lesions in *Ldlr*<sup>-/-</sup> mice.

**Fig. S5.** Effect of *Apoer2* ablation on Reelin-activated monocyte-endothelial cell adhesion.

**Movie S1.** Intravital microscopy displaying leukocyte-endothelial cell adhesion in the mesenteric microcirculation of an *Ldlr*<sup>-/-</sup> mouse.

**Movie S2.** Intravital microscopy displaying leukocyte-endothelial cell adhesion in the mesenteric microcirculation of a DKO mouse.

**Movie S3.** Intravital microscopy displaying leukocyte-endothelial cell adhesion in the mesenteric microcirculation of a vehicle-treated *Reln*<sup>fl/fl</sup>; *Ldlr*<sup>-/-</sup> mouse.

**Movie S4.** Intravital microscopy displaying leukocyte-endothelial cell adhesion in the mesenteric microcirculation of a tamoxifen-treated *Reln*<sup>fl/fl</sup>; *Ldlr*<sup>-/-</sup> mouse.

**Author contributions:** Y.D., L.H., X.X., I.S.Y. performed the experiments and analyzed data, C.R.W. analyzed data and performed statistical analysis, M.F. contributed reagents, C.M., P.W.S. and J.H. supervised the study, P.W.S. and J.H. wrote the paper.

**Competing interests:** Y.D., X.X., C.M., P.W.S., J.H. and University of Texas Southwestern have filed a provisional patent that covers the potential use of anti-Reelin strategies for the prevention of atherosclerosis. The other authors declare that they have no competing interests.

**Data and materials availability:** The CR50 antibody requires a materials transfer agreement from RIKEN.

## Abstract

The multimodular glycoprotein Reelin controls neuronal migration and synaptic transmission by binding to Apolipoprotein E receptor-2 (Apoer2) and very low-density lipoprotein receptor (Vldlr) on neurons. In the periphery, Reelin is produced by the liver, circulates in blood and promotes thrombosis and hemostasis. To investigate if Reelin influences atherogenesis we studied atherosclerosis-prone low-density lipoprotein receptor-deficient (*Ldlr*<sup>-/-</sup>) mice in which we inducibly deleted Reelin either ubiquitously or only in the liver, thus preventing the production of circulating Reelin. In both types of Reelin-deficient mice, atherosclerosis progression was markedly attenuated, and macrophage content and endothelial cell staining for vascular cell adhesion molecule-1 (VCAM1) and intercellular adhesion molecule-1 (ICAM1) were reduced at the sites of atherosclerotic lesions. Intravital microscopy revealed decreased leukocyte-endothelial adhesion in the Reelin-deficient mice. In cultured human endothelial cells, Reelin enhanced monocyte adhesion and increased *ICAM-1*, *VCAM-1* and *E-selectin* expression by suppressing endothelial nitric oxide synthase (eNOS) activity and increasing the activity of NF- $\kappa$ B in an Apoer2-dependent manner. These findings suggest that circulating Reelin promotes atherosclerosis by increasing vascular inflammation, and that reducing or inhibiting circulating Reelin may present a novel approach for the prevention of cardiovascular disease.

## Introduction

Reelin is an extracellular matrix glycoprotein that was originally found in the developing brain where it is secreted by Cajal-Retzius neurons in the marginal zone (1, 2). In neurons, Reelin binds to its cognate receptors Apolipoprotein E receptor 2 (Apoer2) and the very low density lipoprotein receptor (Vldlr) on the cell surface (3), thereby promoting tyrosine phosphorylation of the cytoplasmic adaptor protein disabled homolog 1 (Dab1) (1, 4). Phosphorylated Dab1 then activates a series of signal transduction mechanisms that control various cellular functions, including neuronal positioning during brain development, synaptic plasticity, and memory formation (5). Reelin also regulates lymphatic vessel development (6), interacts with the Notch signaling pathway (7, 8), binds to Ephrins (9, 10) and their Eph ligands (9), and has further been reported to interact with integrins (11–13). Experimental and clinical studies indicate that increased Reelin abundance is protective (14–16), while reduced Reelin abundance in the brain is associated with several neurodegenerative disorders including Alzheimer's disease (AD) (17–20).

In addition to the central nervous system (CNS), Reelin is also present in the circulation, the liver, and some other tissues (21). In the liver, Reelin is produced by stellate cells, not hepatocytes (22). It promotes platelet spreading on fibrinogen and also plays a role in coagulation by enhancing thrombin generation and the formation of fibrin clots (23, 24). There is evidence that the two receptors for Reelin, Apolipoprotein E receptor-2 (Apoer2/Lrp8) and very low-density lipoprotein receptor (Vldlr), influence atherosclerosis severity. In macrophages, Apoer2 reduces stress-induced cell death and potentially retards the development of advanced atherosclerotic plaques (25). In contrast, macrophage Vldlr promotes atherosclerotic lesion development (26). Both Reelin receptors are also present in endothelial cells, where Apoer2 mediates the anti-atherogenic actions of Apolipoprotein E3 (27).

To investigate whether Reelin affects atherosclerosis propensity and whether this involves Reelin binding to its receptors in the periphery, we generated mice with inducible inactivation of Reelin either ubiquitously or selectively only in the circulation. To accelerate atherosclerotic lesion development, Reelin inactivation was performed in LDL receptor-deficient mice (*Ldlr*<sup>-/-</sup>), which are prone to hypercholesterolemia upon feeding a cholesterol-enriched diet (28). We also investigated how Reelin affected leukocyte adhesion to the endothelium and the accumulation of monocytes and macrophages in the vascular wall. Our findings revealed that circulating Reelin promoted the vascular inflammatory response and thus atherosclerosis by increasing leukocyte-endothelial cell adhesion, thereby facilitating the infiltration of inflammatory macrophages into the arterial wall through Apoer2 and the increased expression of mRNAs encoding endothelial adhesion molecules. We further showed that reduction of Reelin in the plasma was sufficient to protect the vascular wall from cholesterol-induced atherosclerosis. Therefore, reducing or inhibiting circulating Reelin, for instance with neutralizing antibodies, siRNA or recombinant decoy receptors, presents a conceptually novel strategy to prevent cardiovascular disease and potentially other disorders that are initiated or promoted by the excessive extravasation of leukocytes or monocytes.

## Results

### Generation and characterization of conditional *Reln*<sup>-/-</sup>;*Ldlr*<sup>-/-</sup> Mice

To explore the potential role of Reelin in the pathogenesis of atherosclerosis, *Ldlr*<sup>-/-</sup> mice were crossed with floxed *Reln* mice expressing a tamoxifen-inducible Cre recombinase under the control of the ubiquitously active CAG promoter. Cre-negative littermates were used as controls. Immunoblot analysis confirmed that tamoxifen injection induced the absence of Reelin protein in the plasma, brains and livers of the double knockout (DKO) mice (Figure S1A). To segregate the potential effects of circulating Reelin on atherosclerosis from those of systemic Reelin, we additionally generated mice with selective deletion of Reelin only in plasma by injecting *Reln*<sup>fl/fl</sup>;*Ldlr*<sup>-/-</sup> mice through the tail vein with adenovirus expressing Cre recombinase (Ad-Cre) or  $\beta$ -galactosidase (Ad-Gal) as control. Immunoblot analysis demonstrated efficient and specific ablation of Reelin from the liver and from plasma, but not from the brain in the Ad-Cre-injected *Reln*<sup>fl/fl</sup>;*Ldlr*<sup>-/-</sup> mice (Figure S2A).

Plasma lipid parameters were determined in all mice after feeding with a high cholesterol diet for 16 weeks. DKO mice and *Ldlr*<sup>-/-</sup> mice had similar body weights, and plasma cholesterol or triglyceride concentrations (Fig. S1B), and the atherogenic diet caused similarly severe hypercholesterolemia with comparable lipid profiles for cholesterol and triglyceride in the two groups of mice (Figure S1C, D). In the adenovirus treated groups, total plasma cholesterol was modestly increased in Ad-Gal *Reln*<sup>fl/fl</sup>;*Ldlr*<sup>-/-</sup> mice compared to Ad-Cre *Reln*<sup>fl/fl</sup>;*Ldlr*<sup>-/-</sup> mice, while plasma triglyceride and HDL-cholesterol (HDL-C) concentrations were similar in the two groups (Figure S2B). Cholesterol feeding had no effect on plasma Reelin concentrations in animals that were wild-type for Reelin (Figure S3).

### Reelin deficiency reduces atherosclerosis in *Ldlr*<sup>-/-</sup> mice

Following high cholesterol feeding for 16 weeks beginning at eight weeks of age, aortas were excised and stained with Oil Red-O to visualize atherosclerotic plaques. En face analyses revealed a 52% decrease in atherosclerotic lesion area in aortas from DKO mice with global Reelin deletion compared to the aortas of control *Ldlr*<sup>-/-</sup> mice (Figure 1A). Quantitative analysis of lesion areas in cross-sections of the aortic sinus showed a similar 47% reduction in lesion size in DKO mice compared to controls (Fig. 1B). Similarly, Ad-Cre *Reln*<sup>fl/fl</sup>;*Ldlr*<sup>-/-</sup> mice displayed a 46% decrease of atherosclerotic lesion area in the aorta and a 73% reduction of aortic root lesions compared with Ad-Gal *Reln*<sup>fl/fl</sup>;*Ldlr*<sup>-/-</sup> mice (Figure 1C and 1D). Thus, both global and plasma-selective Reelin deficiency greatly diminished atherosclerotic lesion formation.

### Reelin deficiency reduces adhesion molecule abundance and macrophage infiltration

We next investigated the presence of macrophages and smooth muscle cells in atherosclerotic plaques from DKO and control *Ldlr*<sup>-/-</sup> mice by immunostaining with antibodies directed against Mac-3 and  $\alpha$ -actin, respectively. Morphometric quantification of the lesions revealed a 32% reduction of Mac-3 positive macrophages in DKO compared to *Ldlr*<sup>-/-</sup> control mice (Fig. 2A). No difference in  $\alpha$ -actin-positive (smooth muscle) area was observed between the two groups.

The migration of monocytes into the subendothelium of arteries in atherosclerosis results from the cytokine-mediated activation of endothelial cells, which leads to increases in the abundance of leukocyte adhesion molecules. To determine the basis for the impact of Reelin on lesion macrophage accumulation, we measured VCAM-1 and ICAM-1 abundance in plaques by immunostaining with antibodies directed against CD106 and CD54 antibodies, respectively. VCAM-1 was reduced by 65% and ICAM-1 by 56% in endothelium overlying plaques in DKO mice compared to *Ldlr*<sup>-/-</sup> mice (Figure 2B). Mac-3, CD106 and CD54 immunoreactivity was similarly reduced in the lesions of Ad-Cre *Reln*<sup>fl/fl</sup>;*Ldlr*<sup>-/-</sup> compared to Ad-Gal *Reln*<sup>fl/fl</sup>;*Ldlr*<sup>-/-</sup> mice (Figure S4). These results suggest that Reelin promotes macrophage foam cell accumulation in atherosclerotic lesions, and that this is likely driven by increased adhesion molecule expression.

### Reelin increases leukocyte-endothelial cell adhesion

Leukocyte recruitment to sites of perivascular inflammation, including atherosclerotic lesions, is a key event in the initiation and progression of vascular injury and repair and enhanced by hypercholesterolemia (29). To better understand the mechanisms by which Reelin promotes macrophage accumulation in atherosclerosis, intravital microscopy was performed to quantify leukocyte-endothelial adhesion *in vivo* in the absence and presence of Reelin. Male DKO and *Ldlr*<sup>-/-</sup> mice were intraperitoneally injected for 5 days with tamoxifen, and the tamoxifen-induced reduction of circulating Reelin was confirmed by Western blotting. Endogenous leukocytes, consisting predominantly of lymphocytes and neutrophils, were fluorescently labeled by injection of Rhodamine-6G, and intravital video microscopy was performed to visualize leukocyte adhesion to the endothelium in the mesenteric microvasculature. Leukocyte velocity was increased by 25% and the number of adherent leukocytes was reduced by 78% in DKO mice compared with *Ldlr*<sup>-/-</sup> mice (Fig. 3,

A and B, and Movies S1, S2). Total circulating white blood cell (WBC) and leukocyte subsets were similar between DKO and *Ldlr*<sup>-/-</sup> mice (Figure 3C), suggesting that Reelin increases leukocyte-endothelial cell adhesion *in vivo*.

To determine if direct actions of Reelin on endothelial cells underlie the apparent increase in adhesion, and if these processes operated in human endothelium, we used U937 cells to investigate monocyte adhesion to cultured primary human aortic endothelial cells (HAECs). Compared with vehicle or mock treated HAECs, Reelin caused a >2-fold increase in adhesion (Figure 4A and 4B), which was completely prevented by the Reelin function-blocking antibody CR50 (Figure 4C) (30, 31). siRNA knockdown of *Vldlr* or *Apoer2* mRNAs was performed to identify the Reelin receptor that mediates the increase in endothelial cell-monocyte adhesion. Whereas loss of *Vldlr* did not alter the effect of Reelin (Figure 4D), *Apoer2* knockdown completely prevented the Reelin mediated increase of endothelial cell-monocyte adhesion (Figure 4D and S5). These results indicate that Reelin enhances adhesion through its action on *Apoer2* and not *Vldlr* in endothelium.

### Reelin antagonizes endothelial NOS through Apoer2

NO generated by endothelial NOS (eNOS) is a key modulator of leukocyte-endothelial cell adhesion (32). Having previously shown that *Apoer2* mediates antiphospholipid antibody-induced suppression of eNOS, which increases endothelial cell-leukocyte adhesion (33), we next determined if Reelin alters eNOS activity in HAECs through *Apoer2*. eNOS activation by VEGF was quantified by measuring <sup>14</sup>C-arginine conversion to <sup>14</sup>C-citrulline in intact HAECs. Whereas VEGF increased eNOS activity in non-treated and mock-treated cells, Reelin partially attenuated eNOS activation (Figure 4E). siRNA knockdown of *Apoer2* fully prevented Reelin-mediated inhibition of eNOS activation. The NO donor S-nitroso-*N*-acetylpenicillamine (SNAP) also completely prevented the Reelin-mediated increase in leukocyte adhesion (Figure 4F). Together, these data show that Reelin signaling to *Apoer2* increases leukocyte adhesion at least in part through reduction of eNOS activity.

### Reelin increases the expression of mRNAs encoding endothelial adhesion proteins

To determine whether Reelin promotes endothelial cell-leukocyte/monocyte adhesion through increased expression of the major endothelial adhesion molecules VCAM-1, ICAM-1, and E-selectin as occurs during atherogenesis (34, 35), we performed quantitative RT-PCR of Mock- and Reelin-treated HAECs. The expression of mRNAs for all three adhesion proteins, which are transcriptionally enhanced during inflammatory conditions, was significantly increased by Reelin treatment, and these increases were prevented by the Reelin function-blocking CR50 antibody (Figure 5A). By contrast, *P-selectin* mRNA expression was not regulated by Reelin under the conditions tested (Figure 5A, rightmost panel). The Reelin-induced increase in *VCAM-1*, *ICAM-1* and *E-selectin* expression was prevented by siRNA knockdown of *Apoer2* (Figure 5B) and by SNAP treatment (Figure 5C), suggesting again an NO sensitive mechanism.

**Reelin increases adhesion molecule expression through NF- $\kappa$ B**—The transcription factor NF- $\kappa$ B is the major driver of *VCAM-1*, *ICAM-1* and *E-selectin* expression (36). Moreover, NO can directly inhibit NF- $\kappa$ B through S-nitrosylation of its

subunits (37) suggesting that the Reelin-mediated increased adhesion molecule gene expression is NF- $\kappa$ B dependent. Indeed, exposure of HAECs to Reelin triggered the rapid phosphorylation and thus inactivation of the endogenous NF- $\kappa$ B inhibitor I $\kappa$ B $\alpha$  (Figure 6A). Conversely, parthenolide, an inhibitor of I $\kappa$ B kinase (38), completely prevented the Reelin-dependent induction of *VCAM-1*, *ICAM-1* and *E-selectin* (Figure 6B–D), confirming that Reelin increases the expression of the mRNAs for these adhesion molecules through activation of the NF- $\kappa$ B signaling pathway.

Taken together, the data we have presented support a model (Figure 7) in which Reelin regulates the expression of major vascular adhesion molecules. This establishes a ‘primed’ state for mounting a rapid reaction to pathological conditions in the vascular wall and the perivascular space that trigger an innate immunity response, such as oxidized LDL or lipopolysaccharides (39).

## Discussion

Reelin, a regulator of brain development and synaptic neuromodulator that signals through ApoE receptors, is also abundant in the liver and present at substantial concentrations in the circulation (21, 23, 24). In the present work, we employed two distinct types of Reelin conditional knockout mice to determine how Reelin affected atherosclerosis. Consistent with earlier studies, our results indicated that the circulating pool of Reelin was peripherally-derived, primarily from the liver, and that it did not originate from the CNS (21). Using these genetic loss-of-function strategies, we found that Reelin potently promoted leukocyte-endothelial adhesion and atherosclerosis in mice.

Arteriosclerosis, thrombosis and inflammatory tissue reactions in general share common vascular response mechanisms that include the recruitment of leukocytes and monocytes to the site of injury, followed by their transmigration into the vascular wall and perivascular space. Although atherosclerosis specifically affects arterial vessels, as opposed to the venous system, and is marked by the subendothelial accumulation of lipids and lipid-laden foam cells (40), it shares the recruitment of circulating leukocytes and monocytes to the developing and progressing lesions with other inflammatory processes that involve the vasculature. Reelin has been reported to affect thrombosis and hemostasis (23, 24). Here we have shown that Reelin promotes atherosclerosis by increasing leukocyte adhesion to the vascular endothelium through increased abundance of the major adhesion molecules that are induced during atherogenesis and which promote the accumulation of macrophages in the lesions - ICAM-1, VCAM-1, and E-selectin (34, 35, 41, 42).

Prior studies of the Reelin receptors Apoer2 and Vldlr in the context of atherosclerosis have investigated cell-autonomous mechanisms of these receptors in macrophages (25, 26). Functional analysis of macrophage Apoer2 in *Ldlr*<sup>-/-</sup> mice suggests that deficiency of the receptor enhances macrophage susceptibility to lipid accumulation and cell death to augment atherosclerotic plaque progression *in vivo* (25). In contrast, the transplantation of Vldlr-positive macrophages into *Vldlr*<sup>-/-</sup> mice markedly accelerates the development of atherosclerotic lesions, suggesting a proatherogenic role of macrophage Vldlr (26). Analysis of cultured macrophages has suggested that the activation of Vldlr and Apoer2 by Reelin or

ApoE3 might increase ABCA1 abundance to promote macrophage cholesterol efflux, thus providing evidence for a potential antiatherogenic role for Reelin (43). Furthermore, the treatment of Vldlr- and Apoer2-overexpressing macrophages with ApoE converts these cells from the proinflammatory M1 to the antiinflammatory M2 phenotype (44), potentially indicating anti-inflammatory actions of the receptors. In contrast to these previous studies, we focused on the ligand for these receptors, and the discrete manipulation of Reelin in mice addressed how this neurodevelopmentally essential ligand, which is also abundantly produced by stellate cells in the liver, promotes atherosclerosis *in vivo* by aggravating vascular inflammation through enhanced macrophage/monocyte adhesion and thus facilitating their subsequent transmigration in response to other chemotactic signals into the vascular wall (Figure 7).

During atherosclerotic lesion development, endothelial dysfunction is an early event that precedes clinical manifestations and complications (45, 46). After activation by proinflammatory cytokines, oxidized lipids or other mediators of the innate immunity response (39), endothelial cells of the vascular wall produce chemokines and adhesion molecules, provoking leukocyte-endothelial cell adhesion, and in turn recruiting inflammatory cells into the lesions (47). *Vldlr* deficiency or endothelial overexpression of Vldlr does not affect atherosclerotic lesion development in *Ldlr* knockout mice, suggesting a modest role at best for Vldlr in endothelial cells in atherogenesis (48). By contrast, we have previously reported that Apoer2 in endothelial cells reduces NO synthesis and promotes leukocyte-endothelial cell adhesion when Apoer2 is mediating the actions of antiphospholipid antibodies, but enhances NO signaling when ApoE3 is the ligand (33, 49). In the present work we showed that hypercholesterolemic *Ldlr*<sup>-/-</sup> mice lacking Reelin either systemically or only in their circulation display decreased staining for vascular adhesion markers (Figure 2), resulting in attenuated leukocyte-endothelial cell adhesion (Figure 3) and reduced atherosclerotic plaque size (Figure 1). We noticed two important differences in the studies in which we used recombinant adenoviruses to delete Reelin selectively in the circulation. First, the total lesion area was greater in the mice that received recombinant adenovirus, either the Ad-Gal control virus or the Ad-Cre virus (Figure 1C), than in the mice in which Cre-mediated recombination was induced with Tamoxifen (Figure 1A). Second, total plasma cholesterol concentrations were somewhat higher in the mice that had received Ad-Gal (Figure S2B), while they were similar in the mice that had received Ad-Cre (Figure S2B) or tamoxifen (Figure S1B). These differences likely reflect the contribution of adenovirus-induced inflammation to the results and highlight a possible common complication of using virus-mediated gene transfer or other invasive manipulations (like bone marrow transplantation) in atherosclerosis experiments. Nevertheless, the results of the adenovirus experiments are consistent with the results obtained in the tamoxifen-treated groups, thereby further supporting the role of Reelin in atherogenesis.

Studies in primary human endothelial cells suggested that the effect of Reelin on the abundance of the major adhesion molecules that mediate leukocyte/monocyte adhesion to the vascular endothelium (Figure 5) underlie its pro-inflammatory actions, and that these likely involve Reelin inhibition of eNOS through Apoer2 (Figure 4) and Reelin-mediated activation of NF- $\kappa$ B (Figure 6). Collectively these observations indicate that the impact of Reelin on atherosclerosis is at least partially caused by its actions on the endothelium.

Our findings are of considerable translational importance, because they suggest a conceptually novel strategy to prevent atherosclerosis and cardiovascular disease. The most effective anti-atherosclerosis therapies to date all target the accumulation of cholesterol in the lesions, by reducing plasma cholesterol either with statins or with antibodies against the LDL receptor antagonist PCSK9 (50, 51). The FDA approved anti-PCSK9 strategies in particular demonstrate the power and ease of systemic antibody application to remove the physiological antagonist (PCSK9) of a beneficial agonist (LDL receptor). In analogy, neutralizing antibodies against Reelin should be similarly beneficial, functioning synergistically by attacking another atherosclerosis promoting mechanism, the endothelial adhesion of blood monocytes. Conceivable alternative strategies involve siRNA- or antisense oligonucleotide-directed ablation of peripheral Reelin production or systemic application of recombinant function-blocking decoy receptors, a strategy that is being successfully employed for anti-TNF therapy (52). In addition, removing or inhibiting circulating Reelin could be expected to further protect against thrombosis by reducing platelet adhesion (23) and clotting propensity (24), factors that also promote atherogenesis. Likewise, suppression of circulating Reelin might also be beneficial in other diseases in which excessive leukocyte/monocyte extravasation contributes to the pathology.

In summary, the conditional Reelin knockout mouse has provided us with a model to study the impact of Reelin on atherosclerosis and the underlying cellular processes. Our cumulative results show that circulating Reelin promotes atherosclerosis development, which is likely attributable to various synergistic molecular mechanisms. These include: (i) the Reelin-induced reduction of eNOS and simultaneous increase of NF- $\kappa$ B activity via Apoer2, resulting in (ii) increased leukocyte-endothelial adhesion and (iii) monocyte/macrophage accumulation in expanding atherosclerotic lesions. These cellular mechanisms, combined with a direct prothrombotic function of Reelin (24), represent peripheral proatherogenic effects of this essential regulator of brain development, synaptic plasticity, learning and memory. Reelin and its surprising modes of action in the context of atherosclerosis open up new avenues to pursue in our efforts to combat cardiovascular disease and potentially other disorders that are driven by excessive leukocyte extravasation.

## Materials and Methods

### Animal models

Mice carrying the loxP-targeted *Reln* gene (which encodes the protein Reelin) were generated by gene targeting murine SV129J ES cells as described previously (15) and mated with *Ldlr*<sup>-/-</sup> (28) mice to yield double homozygotes (*Reln*<sup>fl/fl</sup>;*Ldlr*<sup>-/-</sup>). *Reln*<sup>fl/fl</sup>;*Ldlr*<sup>-/-</sup> mice were then crossbred with *CAG-Cre*<sup>ETR2</sup> mice (Jackson strain # 004682) to obtain *CAG-Cre*<sup>+</sup> *Reln*<sup>fl/fl</sup>;*Ldlr*<sup>-/-</sup> mice and their Cre-negative littermates. To induce Cre-mediated DNA recombination, 6 week-old *Reln*<sup>fl/fl</sup>;*Ldlr*<sup>-/-</sup> mice with or without the *CAG-Cre* transgene were intraperitoneally injected with 0.135 mg/g body weight tamoxifen dissolved in sunflower oil for 5 consecutive days to yield global *Reln* and *Ldlr* double knockout (DKO) mice and *Ldlr*<sup>-/-</sup> (control) mice. To elucidate the role of circulating Reelin in atherogenesis, 6 week-old *Reln*<sup>fl/fl</sup>;*Ldlr*<sup>-/-</sup> mice were intravenously injected with either adenovirus vector encoding Cre recombinase (Ad-Cre) to generate mice lacking

circulating Reelin (Ad-Cre *Reln<sup>fl/fl</sup>;Ldlr<sup>-/-</sup>*), or with adenovirus vector encoding  $\beta$ -galactosidase (Ad-Gal) to generate control mice (Ad-Gal *Reln<sup>fl/fl</sup>;Ldlr<sup>-/-</sup>*). The Ad-Cre and Ad-Gal viruses were produced as described previously (53). Two weeks following injection with either tamoxifen or adenovirus, Reelin concentrations in the plasma, brain and liver were determined by Western blotting. To evaluate atherosclerosis severity, eight-week-old male mice of each genotype, either lacking or expressing Reelin, were placed on an atherogenic high cholesterol diet containing 21% (w/w) milk fat, 1.25% (w/w) cholesterol and 0.5% (w/w) cholic acid (TD 02028, Harlan Laboratories, Indianapolis, IN). In select experiments, WBC counts and differentials were performed by collecting fresh blood obtained through retro-orbital bleeding in EDTA-containing tubes. A ProCyt Dx Hematology Analyzer (IDEXX Laboratories) was used to quantify the five major WBC subpopulations: neutrophils, lymphocytes, monocytes, eosinophils and basophils. All animal procedures were performed according to protocols approved by the Institutional Animal Care and Use Committee at the University of Texas Southwestern Medical Center at Dallas.

### Cell culture and transfection

HAECs (Cambrex Corp.) were cultured in EBM2 medium (Lonza) containing 10% FBS and used within 3–6 passages. The monocyte cell line U937 (human histiocytic lymphoma, ATCC) was grown in RPMI 1640 medium (Sigma-Aldrich) containing 10% FBS. In siRNA experiments, HAECs were transfected using siPORT amine transfection reagent (Life Technologies). Double-stranded siRNA directed against *Vldlr* (s14811) with the functional sequence GCAGUGUAAUGGUAUCCGAtt or *Apoer2* (s15365) with the functional sequence CAUCCCUAAUCUUCACCAAtt were purchased from Life Technologies. Alternative double-stranded siRNA directed against *Apoer2* with the functional sequence CCUUGAAGAUGAUCCACUAUU and control siRNA (D0018100250) were from GE HEALTHCARE DHARMACON INC. The siRNA-mediated silencing of *Apoer2* or *Vldlr* was evaluated by immunoblot analysis.

### Immunoblot analysis

Protein samples from plasma, tissues or HAEC whole cell lysates were prepared in RIPA buffer and separated by SDS-PAGE. After transfer onto nitrocellulose membranes (Bio-Rad), blots were probed separately with antibodies against mouse Reelin (G10), mouse *Apoer2* and *Vldlr* as indicated. The G10 antibody was a generous gift from Andre Goffinet (Université catholique de Louvain, Belgium) (54). The function blocking CR50 antibody was kindly provided by Dr. Katsuhiko Mikoshiba (RIKEN, Saitama, Japan). The *Vldlr* antibody was purchased from Millipore Corporation (Cat #MABS25) and the *Apoer2* antibody was generated in our laboratory as described previously (55). Antibodies against  $\text{I}\kappa\text{B}\alpha$  (Cat #4812) and  $\beta$ -actin (Cat #8457) were purchased from Cell Signaling Technology. Antibody against phospho-Ser<sup>32</sup>/Ser<sup>36</sup>- $\text{I}\kappa\text{B}\alpha$  (Cat #ab12135) was purchased from Abcam. The secondary antibody used was HRP-linked anti-mouse IgG or anti-rabbit IgG (GE Healthcare), and membranes were visualized with SuperSignal West Pico Chemiluminescence reagents and X-ray film. Band intensity was quantified using scanning densitometry of non-saturating autoradiograms with ImageJ software (NIH) within linear exposure range.

### Plasma lipids and lipoprotein profiles

At termination, blood was collected from mice by tail bleeding after an overnight fasting period, and plasma was separated by centrifugation. Plasma lipids (total cholesterol and triglyceride) were determined using kits from Thermo Scientific Company. HDL-cholesterol (HDL-C) was quantified after precipitation of apolipoprotein B-containing lipoproteins with an equal volume of a 20% polyethylene glycol solution as previously described (56). Lipoprotein profiles were determined by fractionation of pooled 500 $\mu$ l plasma from 5 mice in each group using a Superose 6 column (Amersham Pharmacia).

### Atherosclerotic lesion analysis

Mice fed a high cholesterol diet for 16 weeks were euthanized by anesthetic overdose. Hearts were perfused with PBS and 4% paraformaldehyde, and hearts and entire aorta were collected. For en face analysis, entire aortas from the heart extending 5–10 mm beyond the bifurcation of the iliac arteries were removed and dissected free of adjoining tissues, opened, and stained with Oil red O. Lesion extent was evaluated by morphometry of scanned images using ImageJ software. For the analysis of lesions in the aortic sinus, serial cryosections of 10 $\mu$ m thickness were taken from the region of the proximal aorta through the aortic sinuses and stained with Oil red O or hematoxylin. Quantitative immunostaining was performed using primary antibodies against Mac-3 (1:200; BD Pharmingen™),  $\alpha$ -smooth muscle actin (1:200; Abcam), CD106 (1:40; BD Pharmingen™) or CD54 (1:40; R&D systems), and fluorescently-labeled secondary antibodies goat anti-rat Alexa Fluor 488 (ThermoFisher Scientific, A11006), donkey anti-goat Alexa Fluor 594 (ThermoFisher Scientific, A11058), or goat anti-rabbit Alexa Fluor 594 (ThermoFisher Scientific, A11012). Nuclei were counterstained with DAPI (ThermoFisher Scientific, P36935). Images were obtained with a Zeiss Axiophot microscope and the percentage of lesion area that was positively stained was determined using Image-Pro v.6.2 (MediaCybernetics).

### Intravital microscopy for quantification of leukocyte-endothelial cell adhesion

Leukocyte-endothelial adhesion was evaluated as described previously (57). Briefly, 3-week-old male mice were intraperitoneally injected with vehicle or tamoxifen daily for 5 days. After tamoxifen-mediated knockdown of circulating Reelin was confirmed by immunoblotting, the mice were prepared for intravital microscopy. Endogenous leukocytes were fluorescence labeled by injection with Rhodamine-6G (100  $\mu$ l of 0.05% solution given via optic vascular plexus), and the mesentery was exposed for the observation and recording of images of leukocyte adhesion and rolling using a Regita digital camera (QImaging). The velocity and quantity of leukocyte rolling was measured by Image-Pro v.6.2 (MediaCybernetics). In preliminary studies the effects of tamoxifen on adhesion were evaluated in *Reln<sup>fl/fl</sup>;Ldlr<sup>-/-</sup>* mice treated daily for 5 days with tamoxifen or vehicle. WBC velocity was similar in tamoxifen-treated and vehicle-treated mice (see Movies S3 and S4).

### Monocyte adhesion assay

The adhesion of U937 monocytes to monolayers of HAEC was evaluated as previously described (33). Recombinant Reelin and mock conditioned media were collected and purified by column chromatography and size exclusion filtration from the supernatant of

stably-transfected 293 cells and nontransfected 293 cells, respectively (58). Confluent HAECs were treated with vehicle, mock media (20 $\mu$ l per 1 ml), Reelin (20nM) or Reelin (20nM) and CR50 (100nM) for 16h. Subsequently HAEC were washed with PBS and rinsed with RPMI 1640 medium, U937 monocytes (1 $\times$ 10<sup>6</sup> cells/well) were added and incubated with HAEC under rotating conditions (benchtop incubator at 70 rpm) at 37°C for 20min, nonadhered monocytes were removed by gentle washing with PBS, cells were fixed with 1% paraformaldehyde for 10 min at room temperature, and the number of adherent cells was determined in triplicate per  $\times$  40 magnification field by Image J software. In select studies, HAECs were transfected with control, Apoer2 or Vldlr siRNA or treated with 20 $\mu$ M NO donor S-nitroso-*N*-acetylpenicillamine SNAP (Santa Cruz Biotechnology, sc-200319) or with 3 or 10  $\mu$ M Parthenolide (EMD Millipore, Cat #512732) prior to the treatment with mock media or Reelin.

### Endothelial nitric oxide synthase activation assay

Endothelial nitric oxide synthase (eNOS) activation was determined in intact endothelial cells by measuring the conversion of [14C]L-arginine to [14C]l-citrulline as previously described (33). Briefly, HAECs were pretreated with vehicle, mock media or Reelin for 30 min, and eNOS activity was then assessed over 15 min in the continued presence of vehicle, mock media or Reelin (20 nM), in the absence (basal) or presence of VEGF (100 ng/ml). Findings were replicated in 3 or more independent experiments.

### Reverse transcription polymerase chain reaction analysis

RNA was isolated using RNeasy Plus Mini Kit (QIAGEN), and cDNA was prepared by using High Capacity cDNA Reverse Transcription Kit (Applied Biosystems). The expression levels of VCAM1 and ICAM1 in HAECs were measured by RT-PCR on 7900HT Fast Real-time PCR system by using TaqMan Universal Master Mix II (Applied Biosystems) with the following primers: *ICAM-1* (Hs00164932\_m1), *VCAM-1* (Hs01003372\_m1), *HPRT1* (Hs02800695\_m1). *HPRT* expression was used as the internal standard. *P*- and *E*-*Selectin* expression was measured by using *SYBR Green* reagents and following primer sets: Human *P-Selectin* (5'-TGAGCACTGCTTGAAGAAAAGC-3', 5'-CACGTATTCACATTCTGGCCC-3'), Human *E-Selectin* (5'-GGCAGTGGACACAGCAAATC-3', 5'-TGGACAGCATCGCATCTCA-3'), and human acidic ribosomal phosphoprotein protein *36B4* (5'-GGCCTGAGCTCCCTGTCTCT-3', 5'-GCGGTGCGTCAGGGATT-3'), which was used as the internal standard.

### Statistical Analyses

Statistical analyses were performed with Graphpad Prism 6.07 software using one of the following tests: two-tailed unpaired Student's t-test, one-way and two-way ANOVA. All data sets were checked for normality with both the D'Agostino & Pearson omnibus and Shapiro-Wilk normality test or KS normality test (when  $n < 7$  biological replicates or independent experiments). If data was non-normal, a non-parametric test was used to calculate significance. For non-parametric comparisons of two independent groups, a two-tailed Mann-Whitney test was used in place of the Student's t-test. For parametric comparisons of three or more groups, the one-way ANOVA with Sidak's post hoc multiple comparisons test. For non-parametric comparisons of three or more groups, the Kruskal-

Wallis test was performed with Dunn's post hoc multiple comparisons test. For comparison of two or more groups with multiple treatments, the two-way ANOVA test was used with Tukey's or Sidak's post-hoc multiple comparisons test to calculate exact multiplicity adjusted p-values between groups.

## Supplementary Material

Refer to Web version on PubMed Central for supplementary material.

## Acknowledgments

We are indebted to Rebekah Hewitt, Huichuan Reyna, Issac Rocha, Tamara Terrones, Sandy Turner, Emily Boyle, Grant Richards, Nancy Heard and Barbara Dacus for their excellent technical assistance. We thank Andre Goffinet for the G10 antibody and Katsuhiko Mikoshiba for the CR50 antibody.

**Funding:** This work was supported by NIH grant R37 HL063762 (to J.H.) and NIH Grant HL118001 (to P.W.S.). M.F. is a Senior Research Professor of the Hertie Foundation. J.H. was the recipient of an Alexander-von-Humboldt Foundation award during the material steps of this project and was further supported by the American Health Assistance Foundation, the Consortium for Frontotemporal Dementia Research, the Bright Focus Foundation, the Lupe Murchison Foundation, and the Ted Nash Long Life Foundation.

## References

- Hiesberger T, Trommsdorff M, Howell BW, Goffinet A, Mumby MC, Cooper JA, Herz J. Direct binding of Reelin to VLDL receptor and ApoE receptor 2 induces tyrosine phosphorylation of disabled-1 and modulates tau phosphorylation. *Neuron*. 1999; 24:481–489. [PubMed: 10571241]
- Hirota Y, Kubo K, Katayama K, Honda T, Fujino T, Yamamoto TT, Nakajima K. Reelin receptors ApoER2 and VLDLR are expressed in distinct spatiotemporal patterns in developing mouse cerebral cortex. *The Journal of comparative neurology*. 2015; 523:463–478. [PubMed: 25308109]
- Trommsdorff M, Gotthardt M, Hiesberger T, Shelton J, Stockinger W, Nimpf J, Hammer RE, Richardson JA, Herz J. Reeler/Disabled-like disruption of neuronal migration in knockout mice lacking the VLDL receptor and ApoE receptor 2. *Cell*. 1999; 97:689–701. [PubMed: 10380922]
- Fatemi SH. Reelin glycoprotein: structure, biology and roles in health and disease. *Molecular psychiatry*. 2005; 10:251–257. [PubMed: 15583703]
- Durakoglugil MS, Chen Y, White CL, Kavalali ET, Herz J. Reelin signaling antagonizes beta-amyloid at the synapse. *Proceedings of the National Academy of Sciences of the United States of America*. 2009; 106:15938–15943. [PubMed: 19805234]
- Lutter S, Xie S, Tatin F, Makinen T. Smooth muscle-endothelial cell communication activates Reelin signaling and regulates lymphatic vessel formation. *The Journal of cell biology*. 2012; 197:837–849. [PubMed: 22665518]
- Hashimoto-Torii K, Torii M, Sarkisian MR, Bartley CM, Shen J, Radtke F, Gridley T, Sestan N, Rakic P. Interaction between Reelin and Notch signaling regulates neuronal migration in the cerebral cortex. *Neuron*. 2008; 60:273–284. [PubMed: 18957219]
- Sibbe M, Forster E, Basak O, Taylor V, Frotscher M. Reelin and Notch1 cooperate in the development of the dentate gyrus. *The Journal of neuroscience : the official journal of the Society for Neuroscience*. 2009; 29:8578–8585. [PubMed: 19571148]
- Bouche E, Romero-Ortega MI, Henkemeyer M, Catchpole T, Leemhuis J, Frotscher M, May P, Herz J, Bock HH. Reelin induces EphB activation. *Cell research*. 2013; 23:473–490. [PubMed: 23318582]
- Senturk A, Pfennig S, Weiss A, Burk K, Acker-Palmer A. Ephrin Bs are essential components of the Reelin pathway to regulate neuronal migration. *Nature*. 2011; 472:356–360. [PubMed: 21460838]
- Dong E, Caruncho H, Liu WS, Smalheiser NR, Grayson DR, Costa E, Guidotti A. A reelin-integrin receptor interaction regulates Arc mRNA translation in synaptoneuroosomes. *Proceedings of the*

- National Academy of Sciences of the United States of America. 2003; 100:5479–5484. [PubMed: 12707415]
12. Dulabon L, Olson EC, Taglienti MG, Eisenhuth S, McGrath B, Walsh CA, Kreidberg JA, Anton ES. Reelin binds alpha3beta1 integrin and inhibits neuronal migration. *Neuron*. 2000; 27:33–44. [PubMed: 10939329]
  13. Schmid RS, Jo R, Shelton S, Kreidberg JA, Anton ES. Reelin, integrin and DAB1 interactions during embryonic cerebral cortical development. *Cerebral cortex*. 2005; 15:1632–1636. [PubMed: 15703255]
  14. Kramer PL, Xu H, Woltjer RL, Westaway SK, Clark D, Erten-Lyons D, Kaye JA, Welsh-Bohmer KA, Troncoso JC, Markesbery WR, Petersen RC, Turner RS, Kukull WA, Bennett DA, Galasko D, Morris JC, Ott J. Alzheimer disease pathology in cognitively healthy elderly: a genome-wide study. *Neurobiology of aging*. 2011; 32:2113–2122. [PubMed: 20452100]
  15. Lane-Donovan C, Philips GT, Wasser CR, Durakoglugil MS, Masiulis I, Upadhaya A, Pohlkamp T, Coskun C, Kotti T, Steller L, Hammer RE, Frotscher M, Bock HH, Herz J. Reelin protects against amyloid beta toxicity in vivo. *Science signaling*. 2015; 8:ra67. [PubMed: 26152694]
  16. Pujadas L, Rossi D, Andres R, Teixeira CM, Serra-Vidal B, Parcerisas A, Maldonado R, Giralte E, Carulla N, Soriano E. Reelin delays amyloid-beta fibril formation and rescues cognitive deficits in a model of Alzheimer's disease. *Nature communications*. 2014; 5:3443.
  17. Herring A, Donath A, Steiner KM, Widera MP, Hamzehian S, Kanakis D, Kolble K, ElAli A, Hermann DM, Paulus W, Keyvani K. Reelin depletion is an early phenomenon of Alzheimer's pathology. *Journal of Alzheimer's disease : JAD*. 2012; 30:963–979. [PubMed: 22495348]
  18. Knuesel I, Nyffeler M, Mormede C, Muhia M, Meyer U, Pietropaolo S, Yee BK, Pryce CR, LaFerla FM, Marighetto A, Feldon J. Age-related accumulation of Reelin in amyloid-like deposits. *Neurobiology of aging*. 2009; 30:697–716. [PubMed: 17904250]
  19. Beffert U, Weeber EJ, Durudas A, Qiu S, Masiulis I, Sweatt JD, Li WP, Adelman G, Frotscher M, Hammer RE, Herz J. Modulation of synaptic plasticity and memory by Reelin involves differential splicing of the lipoprotein receptor Apoer2. *Neuron*. 2005; 47:567–579. [PubMed: 16102539]
  20. Krstic D, Pfister S, Notter T, Knuesel I. Decisive role of Reelin signaling during early stages of Alzheimer's disease. *Neuroscience*. 2013; 246:108–116. [PubMed: 23632168]
  21. Smalheiser NR, Costa E, Guidotti A, Impagnatiello F, Auta J, Lacor P, Kriho V, Pappas GD. Expression of reelin in adult mammalian blood, liver, pituitary pars intermedia, and adrenal chromaffin cells. *Proceedings of the National Academy of Sciences of the United States of America*. 2000; 97:1281–1286. [PubMed: 10655522]
  22. Samama B, Boehm N. Reelin immunoreactivity in lymphatics and liver during development and adult life. *The anatomical record. Part A, Discoveries in molecular, cellular, and evolutionary biology*. 2005; 285:595–599.
  23. Tseng WL, Huang CL, Chong KY, Liao CH, Stern A, Cheng JC, Tseng CP. Reelin is a platelet protein and functions as a positive regulator of platelet spreading on fibrinogen. *Cellular and molecular life sciences : CMLS*. 2010; 67:641–653. [PubMed: 19936619]
  24. Tseng WL, Chen TH, Huang CC, Huang YH, Yeh CF, Tsai HJ, Lee HY, Kao CY, Lin SW, Liao HR, Cheng JC, Tseng CP. Impaired thrombin generation in Reelin-deficient mice: a potential role of plasma Reelin in hemostasis. *Journal of thrombosis and haemostasis : JTH*. 2014; 12:2054–2064. [PubMed: 25255925]
  25. Waltmann MD, Basford JE, Konaniah ES, Weintraub NL, Hui DY. Apolipoprotein E receptor-2 deficiency enhances macrophage susceptibility to lipid accumulation and cell death to augment atherosclerotic plaque progression and necrosis. *Biochimica et biophysica acta*. 2014; 1842:1395–1405. [PubMed: 24840660]
  26. Eck MV, Oost J, Goudriaan JR, Hoekstra M, Hildebrand RB, Bos IS, van Dijk KW, Van Berkel TJ. Role of the macrophage very-low-density lipoprotein receptor in atherosclerotic lesion development. *Atherosclerosis*. 2005; 183:230–237. [PubMed: 15979629]
  27. Ulrich V, Konaniah ES, Lee WR, Khadka S, Shen YM, Herz J, Salmon JE, Hui DY, Shaul PW, Mineo C. Antiphospholipid antibodies attenuate endothelial repair and promote neointima formation in mice. *Journal of the American Heart Association*. 2014; 3:e001369. [PubMed: 25315347]

28. Ishibashi S, Brown MS, Goldstein JL, Gerard RD, Hammer RE, Herz J. Hypercholesterolemia in low density lipoprotein receptor knockout mice and its reversal by adenovirus-mediated gene delivery. *The Journal of clinical investigation*. 1993; 92:883–893. [PubMed: 8349823]
29. Scalia R, Appel JZ 3rd, Lefer AM. Leukocyte-endothelium interaction during the early stages of hypercholesterolemia in the rabbit: role of P-selectin, ICAM-1, and VCAM-1. *Arteriosclerosis, thrombosis, and vascular biology*. 1998; 18:1093–1100.
30. D'Arcangelo G, Nakajima K, Miyata T, Ogawa M, Mikoshiba K, Curran T. Reelin is a secreted glycoprotein recognized by the CR-50 monoclonal antibody. *The Journal of neuroscience : the official journal of the Society for Neuroscience*. 1997; 17:23–31. [PubMed: 8987733]
31. Utsunomiya-Tate N, Kubo K, Tate S, Kainosho M, Katayama E, Nakajima K, Mikoshiba K. Reelin molecules assemble together to form a large protein complex, which is inhibited by the function-blocking CR-50 antibody. *Proceedings of the National Academy of Sciences of the United States of America*. 2000; 97:9729–9734. [PubMed: 10920200]
32. Kubes P, Suzuki M, Granger DN. Nitric oxide: an endogenous modulator of leukocyte adhesion. *Proceedings of the National Academy of Sciences of the United States of America*. 1991; 88:4651–4655. [PubMed: 1675786]
33. Ramesh S, Morrell CN, Tarango C, Thomas GD, Yuhanna IS, Girardi G, Herz J, Urbanus RT, de Groot PG, Thorpe PE, Salmon JE, Shaul PW, Mineo C. Antiphospholipid antibodies promote leukocyte-endothelial cell adhesion and thrombosis in mice by antagonizing eNOS via beta2GPI and apoER2. *The Journal of clinical investigation*. 2011; 121:120–131. [PubMed: 21123944]
34. Galkina E, Ley K. Leukocyte influx in atherosclerosis. *Current drug targets*. 2007; 8:1239–1248. [PubMed: 18220701]
35. Galkina E, Ley K. Vascular adhesion molecules in atherosclerosis. *Arteriosclerosis, thrombosis, and vascular biology*. 2007; 27:2292–2301.
36. Chen CC, Rosenbloom CL, Anderson DC, Manning AM. Selective inhibition of E-selectin, vascular cell adhesion molecule-1, and intercellular adhesion molecule-1 expression by inhibitors of I kappa B-alpha phosphorylation. *Journal of immunology*. 1995; 155:3538–3545.
37. Qian J, Fulton DJ. Exogenous, but not Endogenous Nitric Oxide Inhibits Adhesion Molecule Expression in Human Endothelial Cells. *Frontiers in physiology*. 2012; 3:3. [PubMed: 22279436]
38. Saadane A, Masters S, DiDonato J, Li J, Berger M. Parthenolide inhibits IkappaB kinase, NF-kappaB activation, and inflammatory response in cystic fibrosis cells and mice. *American journal of respiratory cell and molecular biology*. 2007; 36:728–736. [PubMed: 17272824]
39. Yan ZQ, Hansson GK. Innate immunity, macrophage activation, and atherosclerosis. *Immunological reviews*. 2007; 219:187–203. [PubMed: 17850490]
40. Lu H, Daugherty A. Atherosclerosis. *Arteriosclerosis, thrombosis, and vascular biology*. 2015; 35:485–491.
41. Johnson RC, Chapman SM, Dong ZM, Ordovas JM, Mayadas TN, Herz J, Hynes RO, Schaefer EJ, Wagner DD. Absence of P-selectin delays fatty streak formation in mice. *The Journal of clinical investigation*. 1997; 99:1037–1043. [PubMed: 9062362]
42. Stannard AK, Riddell DR, Sacre SM, Tagalakis AD, Langer C, von Eckardstein A, Cullen P, Athanasopoulos T, Dickson G, Owen JS. Cell-derived apolipoprotein E (ApoE) particles inhibit vascular cell adhesion molecule-1 (VCAM-1) expression in human endothelial cells. *The Journal of biological chemistry*. 2001; 276:46011–46016. [PubMed: 11590165]
43. Chen X, Guo Z, Okoro EU, Zhang H, Zhou L, Lin X, Rollins AT, Yang H. Up-regulation of ATP binding cassette transporter A1 expression by very low density lipoprotein receptor and apolipoprotein E receptor 2. *The Journal of biological chemistry*. 2012; 287:3751–3759. [PubMed: 22170052]
44. Baitsch D, Bock HH, Engel T, Telgmann R, Muller-Tidow C, Varga G, Bot M, Herz J, Robenek H, von Eckardstein A, Nofer JR. Apolipoprotein E induces antiinflammatory phenotype in macrophages. *Arteriosclerosis, thrombosis, and vascular biology*. 2011; 31:1160–1168.
45. Choi BJ, Matsuo Y, Aoki T, Kwon TG, Prasad A, Gulati R, Lennon RJ, Lerman LO, Lerman A. Coronary endothelial dysfunction is associated with inflammation and vasa vasorum proliferation in patients with early atherosclerosis. *Arteriosclerosis, thrombosis, and vascular biology*. 2014; 34:2473–2477.

46. Mudau M, Genis A, Lochner A, Strijdom H. Endothelial dysfunction: the early predictor of atherosclerosis. *Cardiovascular journal of Africa*. 2012; 23:222–231. [PubMed: 22614668]
47. Hansson GK, Libby P. The immune response in atherosclerosis: a double-edged sword. *Nature reviews. Immunology*. 2006; 6:508–519.
48. Tacke PJ, Delsing DJ, Gijbels MJ, Quax PH, Havekes LM, Hofker MH, van Dijk KW. VLDL receptor deficiency enhances intimal thickening after vascular injury but does not affect atherosclerotic lesion area. *Atherosclerosis*. 2002; 162:103–110. [PubMed: 11947903]
49. Ulrich V, Konaniah ES, Herz J, Gerard RD, Jung E, Yuhanna IS, Ahmed M, Hui DY, Mineo C, Shaul PW. Genetic variants of ApoE and ApoER2 differentially modulate endothelial function. *Proceedings of the National Academy of Sciences of the United States of America*. 2014; 111:13493–13498. [PubMed: 25197062]
50. Horton JD, Cohen JC, Hobbs HH. PCSK9: a convertase that coordinates LDL catabolism. *Journal of lipid research*. 2009; 50(Suppl):S172–S177. [PubMed: 19020338]
51. Stein EA, Mellis S, Yancopoulos GD, Stahl N, Logan D, Smith WB, Lisbon E, Gutierrez M, Webb C, Wu R, Du Y, Kranz T, Gasparino E, Swergold GD. Effect of a monoclonal antibody to PCSK9 on LDL cholesterol. *The New England journal of medicine*. 2012; 366:1108–1118. [PubMed: 22435370]
52. Peppel K, Crawford D, Beutler B. A tumor necrosis factor (TNF) receptor-IgG heavy chain chimeric protein as a bivalent antagonist of TNF activity. *The Journal of experimental medicine*. 1991; 174:1483–1489. [PubMed: 1660525]
53. Rohlmann A, Gotthardt M, Willnow TE, Hammer RE, Herz J. Sustained somatic gene inactivation by viral transfer of Cre recombinase. *Nature biotechnology*. 1996; 14:1562–1565.
54. de Bergeyck V, Naerhuyzen B, Goffinet AM, Lambert de Rouvroit C. A panel of monoclonal antibodies against reelin, the extracellular matrix protein defective in reeler mutant mice. *Journal of neuroscience methods*. 1998; 82:17–24. [PubMed: 10223511]
55. Beffert U, Durudas A, Weeber EJ, Stolt PC, Giehl KM, Sweatt JD, Hammer RE, Herz J. Functional dissection of Reelin signaling by site-directed disruption of Disabled-1 adaptor binding to apolipoprotein E receptor 2: distinct roles in development and synaptic plasticity. *The Journal of neuroscience : the official journal of the Society for Neuroscience*. 2006; 26:2041–2052. [PubMed: 16481437]
56. Ding Y, Zhang L, Wang Y, Huang W, Tang Y, Bai L, Ross CJ, Hayden MR, Liu G. Amelioration of hypertriglyceridemia with hypo-alpha-cholesterolemia in LPL deficient mice by hematopoietic cell-derived LPL. *PloS one*. 2011; 6:e25620. [PubMed: 21980507]
57. Umetani M, Ghosh P, Ishikawa T, Umetani J, Ahmed M, Mineo C, Shaul PW. The Cholesterol Metabolite 27-Hydroxycholesterol Promotes Atherosclerosis via Proinflammatory Processes Mediated by Estrogen Receptor Alpha. *Cell Metab*. 2014
58. Beffert U, Morfini G, Bock HH, Reyna H, Brady ST, Herz J. Reelin-mediated signaling locally regulates protein kinase B/Akt and glycogen synthase kinase 3beta. *The Journal of biological chemistry*. 2002; 277:49958–49964. [PubMed: 12376533]

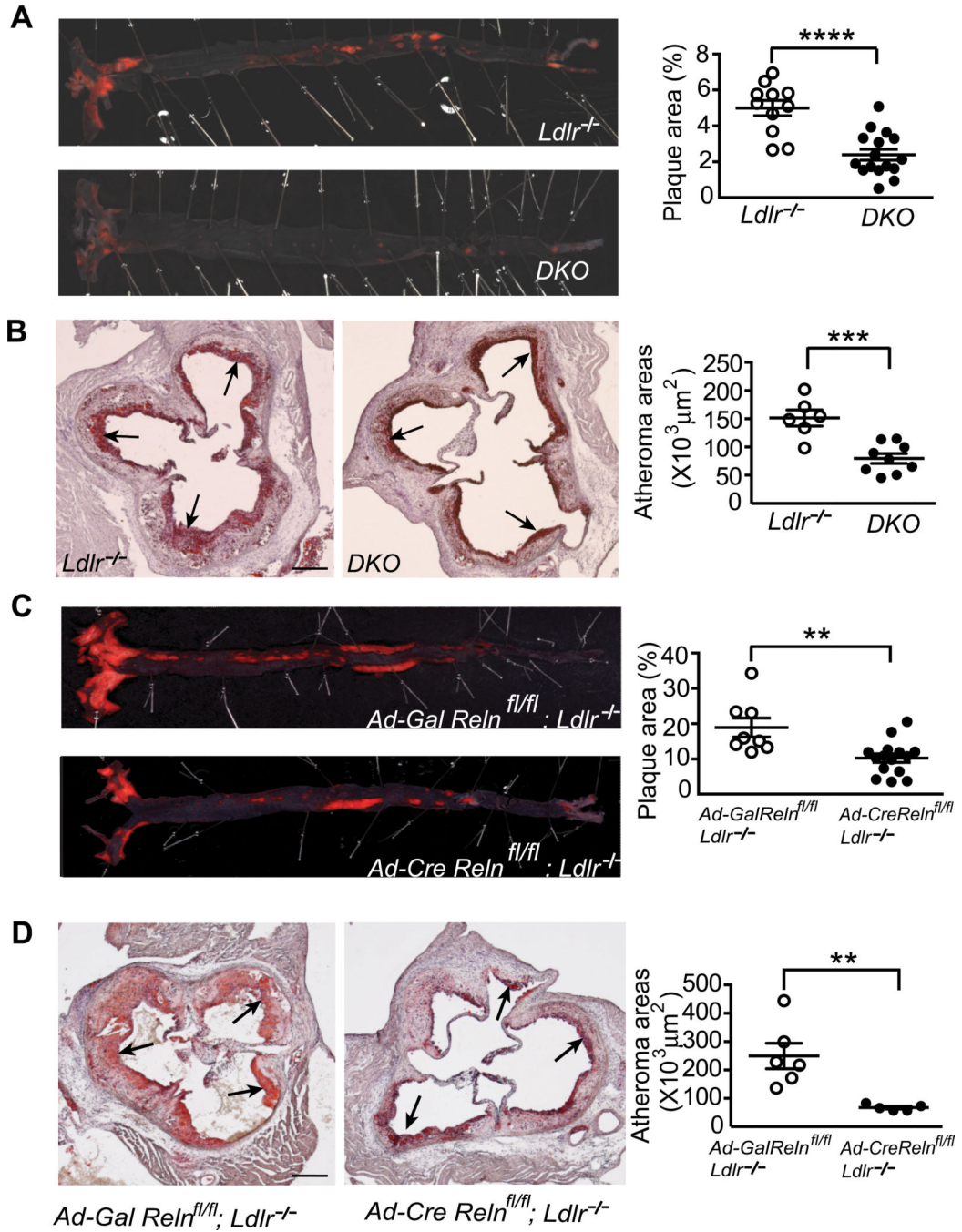


**Fig. 1. Reelin deficiency attenuates atherosclerotic lesion development in *Ldlr<sup>-/-</sup>* mice**  
 (A) Representative en face photomicrographs (*left*) and average percent of aortic lesion area in male *Ldlr<sup>-/-</sup>* (n=11 animals) and *DKO* (n=16 animals) mice (*right*, \*\*\*\*P<0.0001). (B) Representative photomicrographs of aortic root sections stained with Oil Red O (*left*) and quantification of atheroma area in *Ldlr<sup>-/-</sup>* (n=6 animals) and *DKO* (n=9 animals) (*right*, \*\*\*P=0.0005). (C) Representative en face photomicrographs (*left*) and average percent of aortic lesion area in *Ad-Cre-Reln<sup>fl/fl</sup> Ldlr<sup>-/-</sup>* (n=8 animals) and *Ad-Gal-Reln<sup>fl/fl</sup> Ldlr<sup>-/-</sup>* (n=15 animals) mice (*right*, \*\*P=0.0029). (D) Representative photomicrographs of aortic

root sections stained with Oil Red O (*left*) and quantification of the atheroma area in *Ad-Cre-Reln<sup>fl/fl</sup> Ldlr<sup>-/-</sup>* (n=6 animals) and *Ad-Gal-Reln<sup>fl/fl</sup> Ldlr<sup>-/-</sup>* (n=15 animals) (*right*, \*\*P=0.0053). Summary plots depict the mean  $\pm$  SEM. Additional statistical details are summarized in Table S1.

Author Manuscript

Author Manuscript

Author Manuscript

Author Manuscript

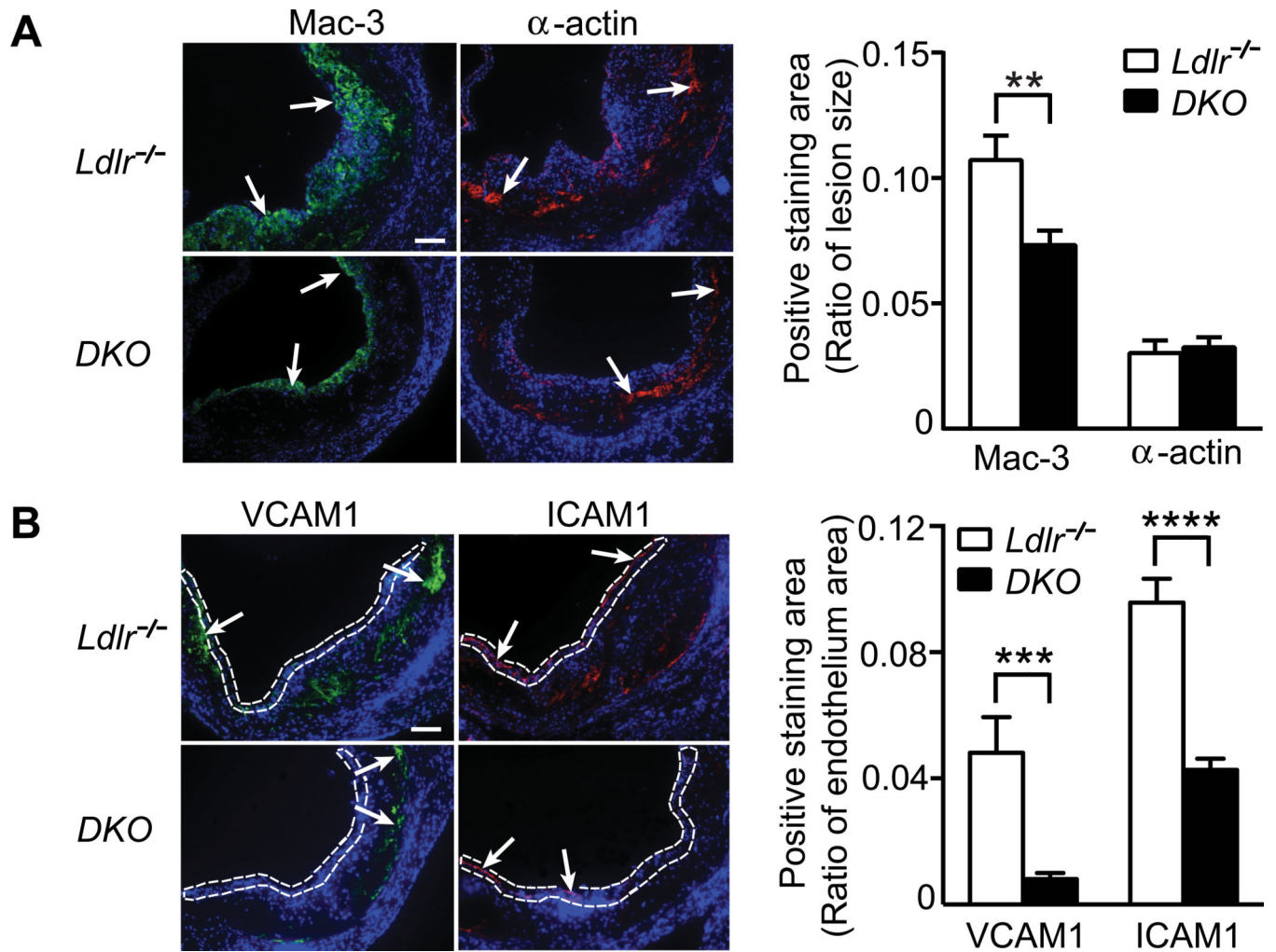


**Fig. 2. global Reelin deficiency decreases monocyte recruitment to atherosclerotic lesions in *Ldlr*<sup>-/-</sup> mice**

(A) Representative aortic root cross-sections from *Ldlr*<sup>-/-</sup> and *DKO* mice stained with specific antibodies for macrophages (Mac-3 protein, green) and smooth muscle cells ( $\alpha$ -actin protein, red) (*left*) and the average positive staining (*right*, normalized to lesion area) for Mac-3 (\* $P=0.0349$ ) and  $\alpha$ -actin ( $P=0.7612$ ). (B) Representative aortic sinus sections from *Ldlr*<sup>-/-</sup> and *DKO* mice stained with specific antibodies for VCAM1 (green) and ICAM1 (red) (*left*) and the average positive staining (*right*, normalized to endothelium area, as indicated by white dotted line) for VCAM1 (\* $P=0.0301$ ) and ICAM1 (\*\*\*\* $P=0.0012$ ). In panels A and B, sections were counterstained with DAPI (blue) to stain nuclei. White arrows indicate positive staining and summary plots represent the mean  $\pm$  SEM ( $n=6-7$  animals/genotype; average of 3-6 sections/animal). Additional statistical details are summarized in Table S1.

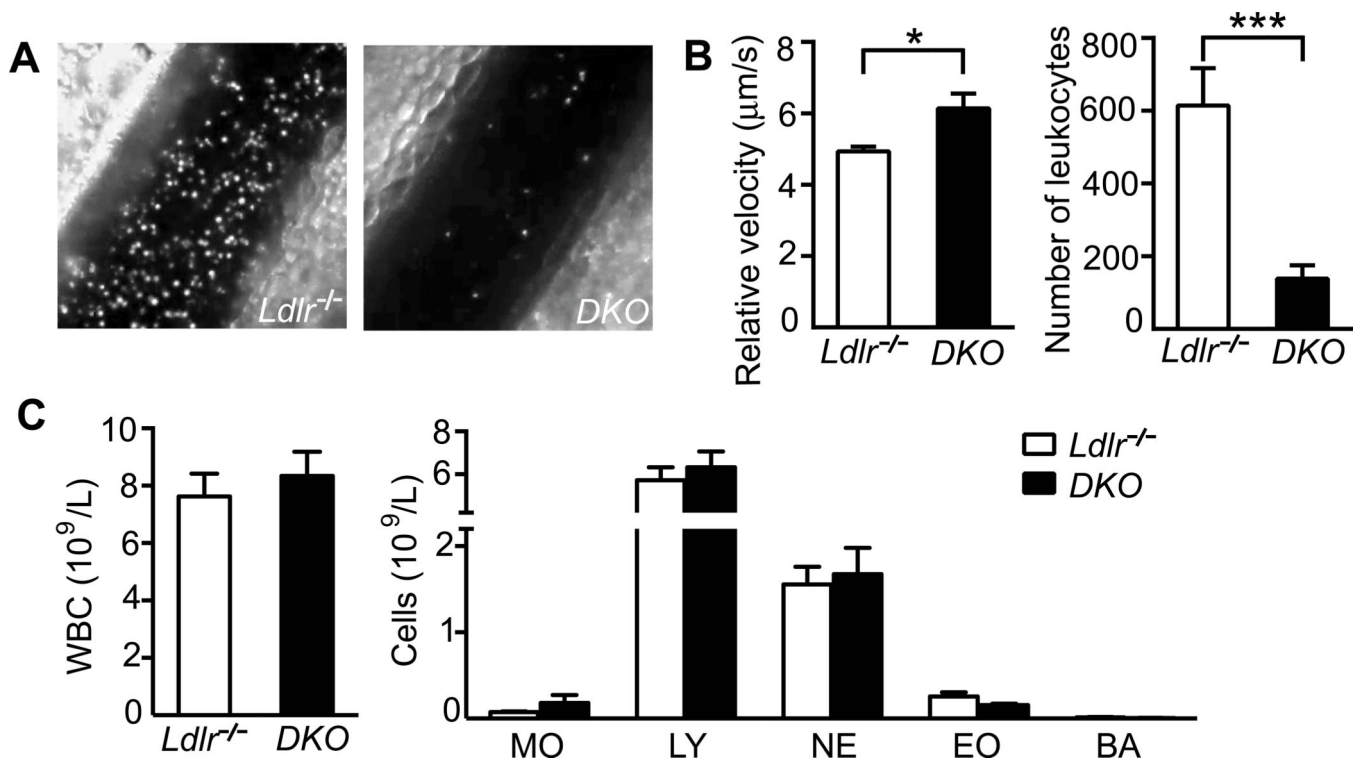


**Fig. 3. Global Reelin deficiency reduces leukocyte-endothelial cell adhesion, and it has no effect on circulating WBC number**

(A) Representative images of leukocyte-endothelial cell adhesion in the mesenteric microcirculation in male *Ldlr*<sup>-/-</sup> and *DKO* after peritoneal injection of tamoxifen daily for 5 days. (B) Summary plots depicting the average leukocyte velocity (*left*, \**P*=0.0136) and the number of adherent leukocytes (*right*, \*\*\**P*=0.0003) in *Ldlr*<sup>-/-</sup> and *DKO* mice (*n*=10 animals/genotype). (C) Summary graphs depicting the average total white blood cell count (WBC, *P*=0.5524) and average number of leukocyte subtypes in plasma from *Ldlr*<sup>-/-</sup> (*n*=6 animals) and *DKO* (*n*=7 animals) mice (MO, monocyte; LY, lymphocyte; NE, neutrophils; EO, eosinophil; BA, basophil) (not significant). Summary plots depict the mean ± SEM. Additional statistical details are summarized in Table S1.

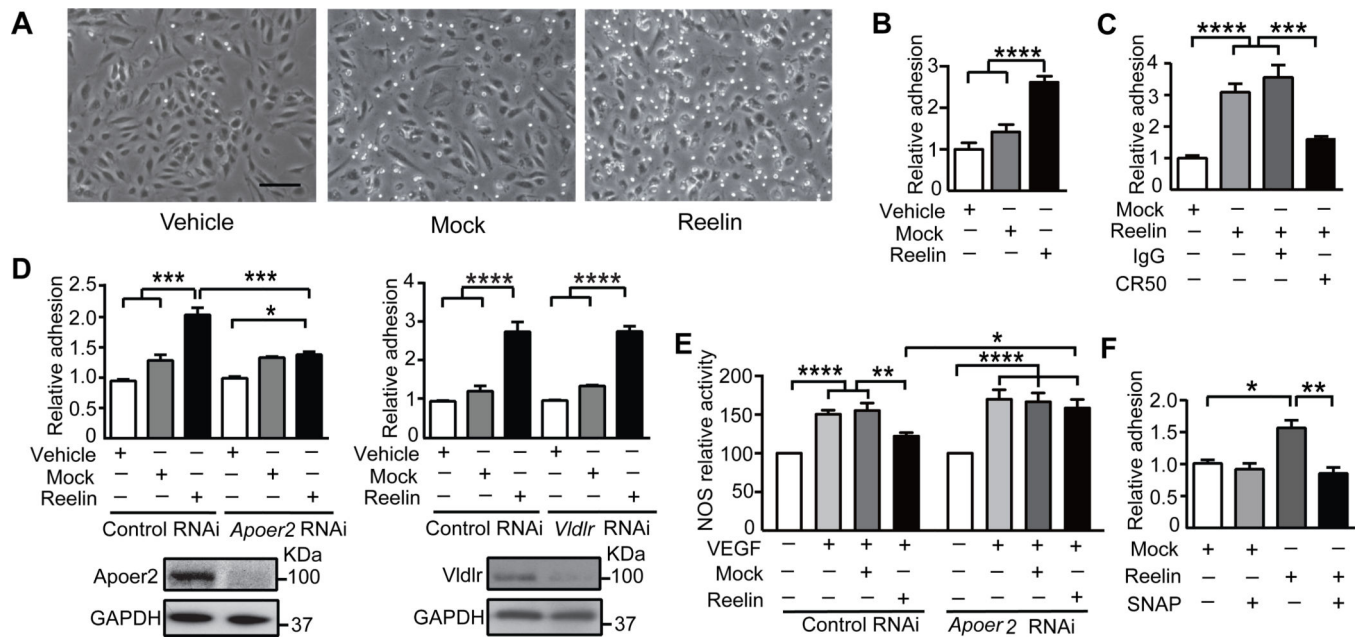


**Fig. 4. Reelin enhances monocyte-endothelial cell adhesion and blunts VEGF-induced eNOS activation via Apoer2**

(A) Representative images of U937 monocytes (small, round cells) adhered to HAEC endothelial cells (cobblestone shape) treated with vehicle, mock or Reelin (scale bar=200 $\mu$ m). (B-F) Summary plots depicting the mean $\pm$ SEM of the following: (B) Number of adhered monocytes per 40X-field-of-view in (A) (n=6 independent experiments, \*\*\*\*P<0.0001). (C) Monocyte-HAEC adhesion with mock, Reelin  $\pm$  mouse IgG or CR50 (n=6 independent experiments; \*\*\*P<0.002, \*\*\*\*P<0.0001). (D) Monocyte-HAEC adhesion with vehicle, mock or Reelin (top) after transfection with either control (control RNAi), double-stranded RNA targeting *Apoer2* (left, n=3 independent experiments; \*\*\*\*P<0.0001) or *Vldlr* (right, n=3 independent experiments; \*\*\*\*P<0.0009). In parallel, whole cell lysates were immunoblotted for Vldlr or Apoer2 and GAPDH (bottom). (E) VEGF-stimulated eNOS activity in HAECs with or without Apoer2 knockdown, pre-treated with or without mock or Reelin (n=6 independent experiments; \*P<0.02; \*\*P<0.006; \*\*\*\*P<0.0001). (F) Monocyte-HAEC adhesion in the presence of mock or Reelin  $\pm$  SNAP (n=6 independent experiments, \*\*P=0.0081, \*\*\*\*P=0.0001). The concentrations used were as follows: Reelin, 20nM; mouse IgG, 100nM; CR50, 100nM; SNAP, 20 $\mu$ M. Additional statistical details are summarized in Table S1.

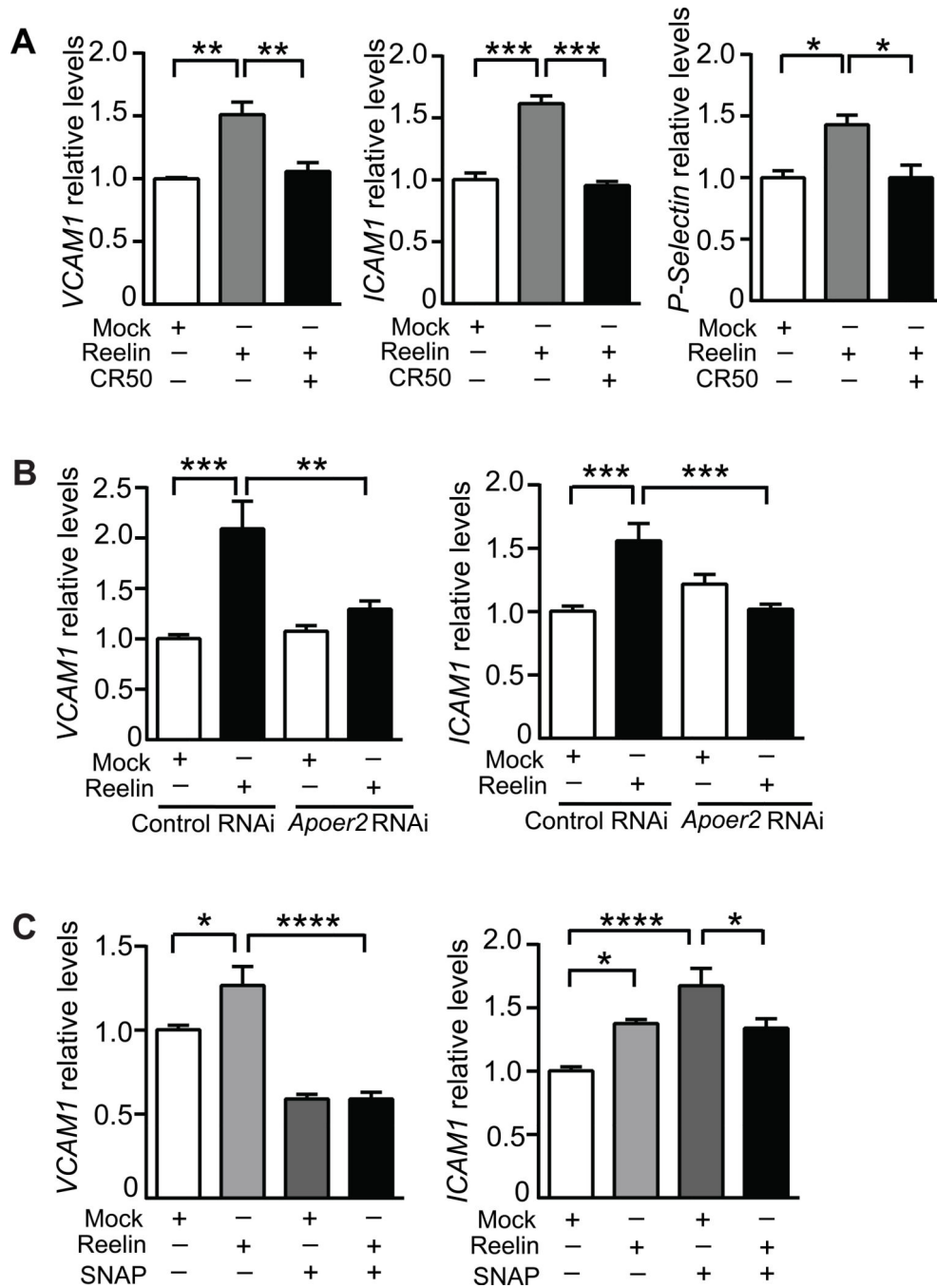


**Fig. 5. Reelin activates endothelial adhesion molecules expression in HAECs**

(A) Summary plots depicting the relative transcript abundance of *VCAM1* (left,  $**P < 0.01$ ), *ICAM1* relative to *HPRT1* (middle left,  $***P < 0.0005$ ), *E-Selectin* (middle right,  $***P = 0.0014$ ,  $***P = 0.0005$ ) and *P-Selectin* relative to *36B4* (right, not significant) in HAECs treated with mock or Reelin±CR50 for 16h evaluated by RT-PCR (n=3 or more independent experiments). (B) qPCR for the expression of *VCAM1* (left, n=6,  $**P = 0.002$ ,  $***P = 0.0005$ ), *ICAM1* (middle,  $***P < 0.002$ ) and *E-Selectin* (right,  $**P = 0.0088$ ,  $***P = 0.0007$ ) in HAECs treated with mock or Reelin after transfection with either control

(control RNAi) or double-stranded RNA targeting *Apoer2* (left, middle, n=6; right, n=3 independent experiments). (C) qPCR for the expression of *VCAM1* (left, no SNAP: \*\*P=0.0043; right, SNAP: P=0.9964), (D) *ICAM1* (left, no SNAP: \*\*\*\*P<0.0001; right, SNAP: P=0.0579), and (E) *E-Selectin* (left, no SNAP: \*\*P=0.0021; right, SNAP: P=0.0861) in HAECs treated with mock or Reelin ± SNAP for 16h (n=6 independent experiments). The concentrations used were as follows: Reelin, 20nM; mouse IgG, 100nM; CR50, 100nM; SNAP, 20μM. Summary plots depict the mean ± SEM. Additional statistical details are summarized in Table S1.

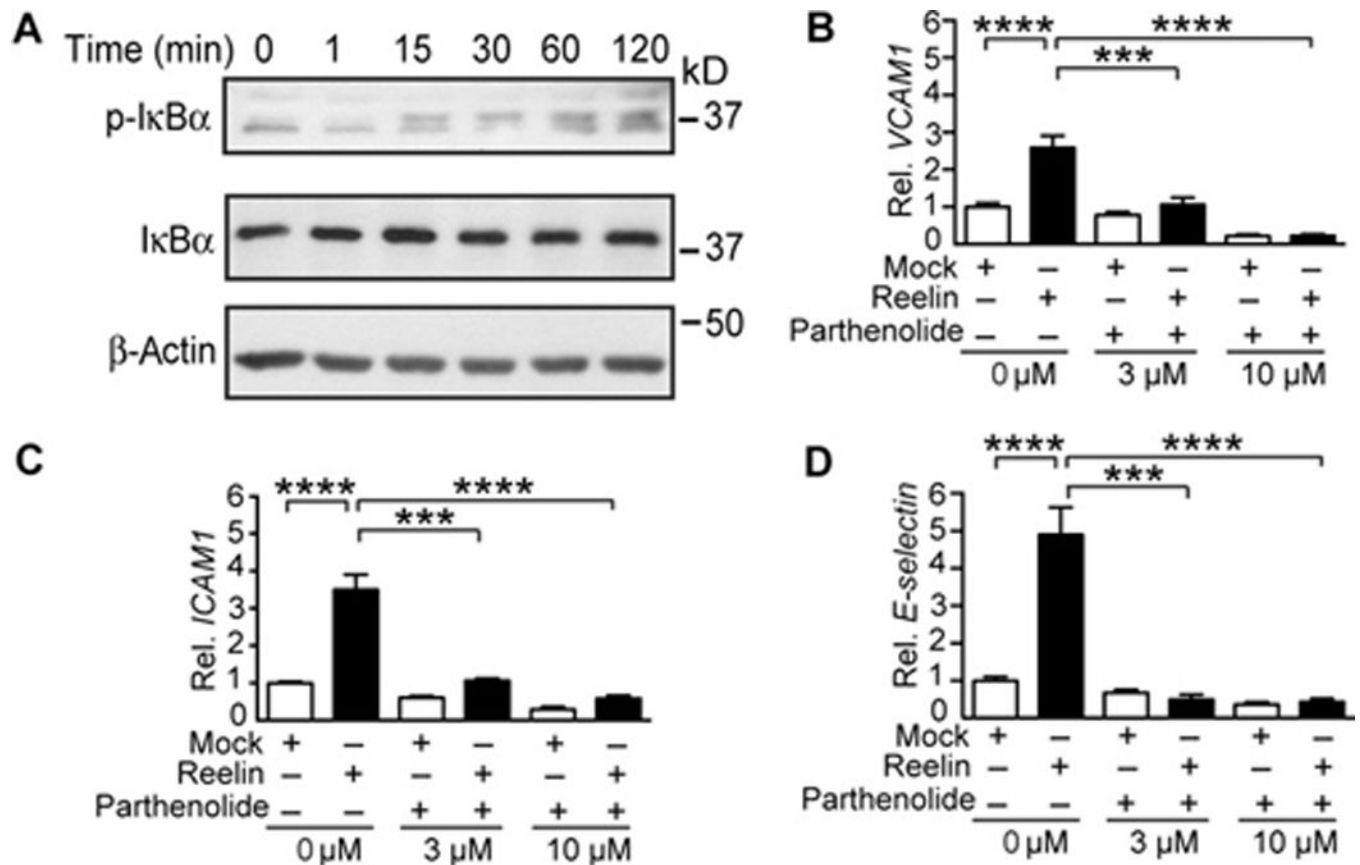


**Fig. 6. Reelin induces IkB $\alpha$  phosphorylation and activates NF- $\kappa$ B in HAECs**

(A) Representative western blot shows the effect of Reelin (20nM) on the phosphorylation of IkB $\alpha$  (the upper and lower bands represent phospho-IkB $\alpha$  and non-phospho-IkB $\alpha$ , respectively) in HAECs. Incubations were terminated at the indicated time-points after addition of purified Reelin or medium. (B–D) qPCR for the expression of *VCAM1* (B) (\*\*\*\*P<0.0001), *ICAM1* (C) (\*\*\*P=0.0003, \*\*\*\*P<0.0001), and *E-Selectin* (D) (\*\*\*\*P<0.0001) in HAECs treated with mock or Reelin with or without 3 $\mu$ M, 10 $\mu$ M parthenolide. (n=3–16 replicates per treatment over 3 independent experiments). Summary plots depict the mean  $\pm$  SEM. Additional statistical details are summarized in Table S1.

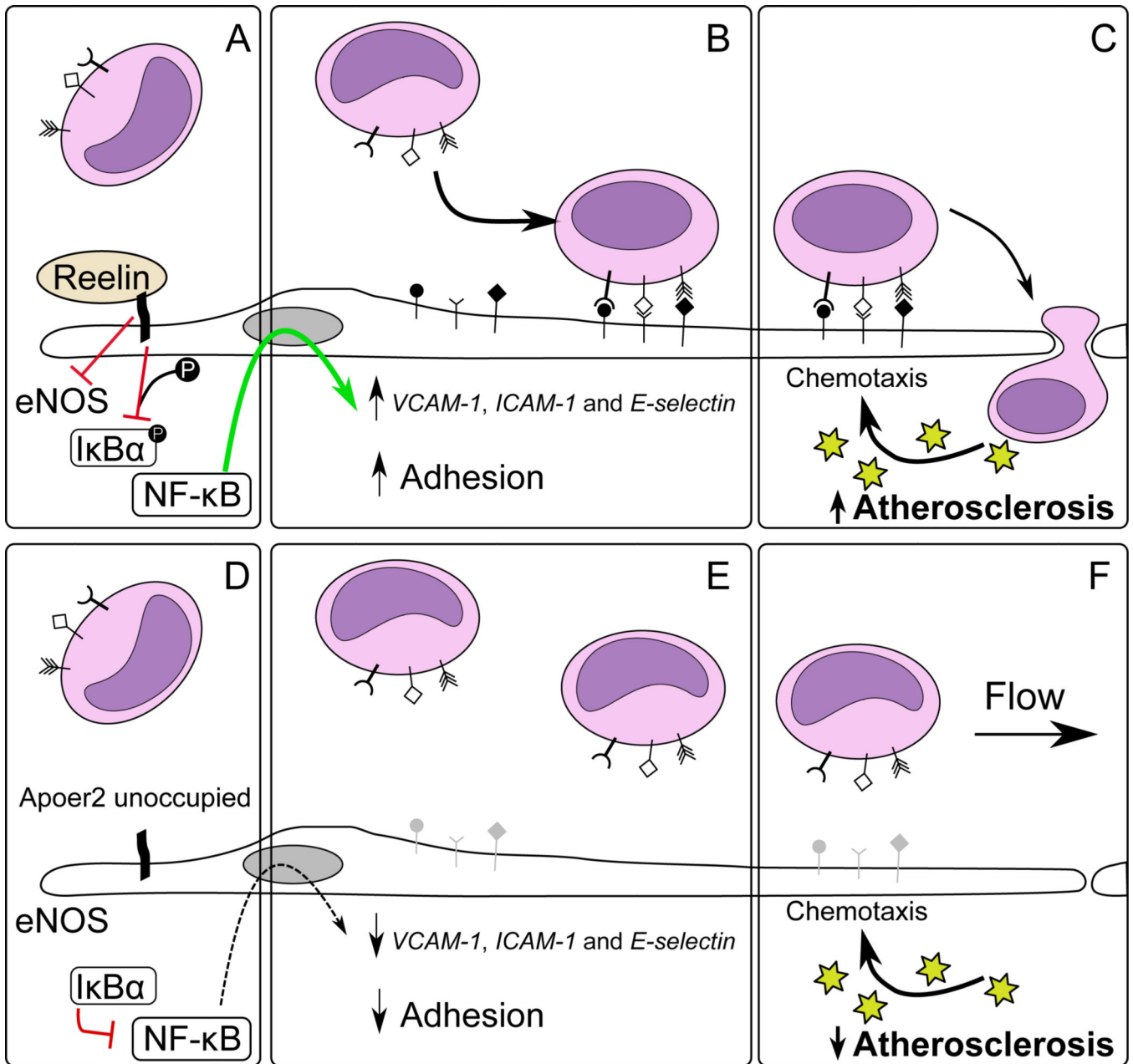


**Fig. 7. Model of Reelin actions on the vascular endothelium**

(A) In the presence of circulating Reelin, endothelial Apoer2 attenuates eNOS and induces the phosphorylation of I $\kappa$ B $\alpha$ , which prevents I $\kappa$ B $\alpha$  from inhibiting NF- $\kappa$ B, a transcription factor that (B) increases the expression of the vascular adhesion molecules VCAM-1, ICAM-1 and E-selectin. This results in the prolonged attachment of circulating leukocytes and monocytes and improves their surveillance of vascular and perivascular health by increasing their receptiveness to (C) chemotactic or inflammatory stimuli emanating from the subendothelial space (e.g. oxidized LDL, symbolized by the *yellow stars*), thereby indirectly increasing the likelihood of initiating diapedesis. (D) In the absence of Reelin, Apoer2 is unoccupied, eNOS is not attenuated, and I $\kappa$ B $\alpha$  is not phosphorylated and thus

able to inhibit NF- $\kappa$ B. **(E)** Consequently, the relative expression of the NF-kB responsive adhesion molecules is reduced (symbolized by their light gray color) and attachment of circulating leukocytes/monocytes is diminished. **(F)** The reduced opportunity to interact with adhesion molecules diminishes the likelihood of a passing leukocyte/monocyte to productively engage the vascular wall and initiate diapedesis in response to chemotactic signals, resulting in reduced macrophage accumulation and atherosclerosis.

Author Manuscript

Author Manuscript

Author Manuscript

Author Manuscript